

# Strain-induced ordering of microdomain structures in polystyrene-*block*-polybutadiene-*block*-polystyrene triblock copolymers cross-linked in the disordered state

Sakae Aida, Shinichi Sakurai\*, Shunji Nomura

Department of Polymer Science and Engineering, Kyoto Institute of Technology, Matsugasaki, Sakyo-ku, Kyoto 606-8585, Japan

Received 17 August 2001; received in revised form 29 November 2001; accepted 6 December 2001

## Abstract

Strain-induced ordering of microdomain structures in cross-linked polystyrene-*block*-polybutadiene-*block*-polystyrene (SBS) triblock copolymers was examined by the small-angle X-ray scattering technique. To stretch the SBS samples at elevated temperature above the glass transition temperature of polystyrene, polybutadiene blocks were chemically cross-linked in the disordered state. The initial morphology was disorder-like or bicontinuous due to incompleteness of microphase separation in the presence of the chemical cross-links. When the cross-linked SBS samples were mechanically stretched at 130 °C and were further annealed for 24 h under a stretched state, the random domain structures ordered gradually and lamellar-like regularity was finally attained. It was found that the ordering proceeded more for the case of the higher strain. © 2002 Elsevier Science Ltd. All rights reserved.

**Keywords:** Strain-induced ordering; Cross-linked polystyrene-*block*-polybutadiene-*block*-polystyrene triblock copolymer; Small-angle X-ray scattering

## 1. Introduction

Block copolymers undergo microphase separation and form well-ordered microdomain structures, such as spheres, cylinders, and lamellae. The microdomain structures can be controlled by composition, temperature, and other factors [1–4]. It is well known that microdomain structures govern macroscopic physical properties [5–10]. The mechanical properties of block copolymers consisting of glassy and rubbery blocks depend on the composition. If the content of glassy blocks is lower, the block copolymer exhibits the elastomeric properties, since glassy microdomains act as physical cross-links for the rubbery matrix and they are used as thermoplastic elastomers [5]. When the content is higher, the block copolymers are used as impact-resistant or shrinkable materials. The mechanical properties also depend on the orientation of microdomain structures, which is especially responsible for anisotropic properties. By applying extensional or dynamic shear flow, the microdomain structure can be highly aligned. In recent years, many experimental works have been reported on the strain-induced orientation of lamellar [11–14], cylindrical [15–20], and spherical microdomains [21,22]. It is also

interesting to further explore the possibility of strain-induced morphological or structural change.

In this study, we conducted experiments to examine the strain-induced ordering of microdomain structures in polystyrene-*block*-polybutadiene-*block*-polystyrene (SBS) triblock copolymers with simple extensional flow. For this purpose, we stretched the sample at elevated temperatures above the glass transition temperature ( $T_g$ ) of the polystyrene (PS) block chains. To stretch the sample at temperatures above  $T_g$  of PS ( $T_{g,PS}$ ), the polybutadiene (PB) chains were chemically cross-linked. We have already investigated microdomain structures and mechanical properties of SBS triblock copolymers of which PB blocks are chemically cross-linked in the disordered state [23,24]. For those studies, after a lamellar forming SBS triblock copolymer was chemically cross-linked in the disordered state (in the presence of solvent), the cross-linked sample was subjected to microphase separation by extracting the solvent. We have analyzed microdomain structures for this sample, using the small-angle X-ray scattering (SAXS) technique and the transmission electron microscopy, and found ill-ordered microdomain structures with a bicontinuous feature, which is far different from the original lamellar structures in the absence of cross-links [23]. It was, however, revealed in the present study that such the microdomains ordered, when the cross-linked samples were stretched at temperatures

\* Corresponding author. Tel.: +81-75-724-7864; fax: +81-75-724-7800.  
E-mail address: shin@ipc.kit.ac.jp (S. Sakurai).

higher than the  $T_{g,PS}$ , where the samples were annealed for several hours at the stretched state. We discuss the effect of strain on the degree of ordering of the microdomain structures.

## 2. Experimental

### 2.1. Sample preparation

The SBS triblock copolymer (code name: TR2400 supplied by Japan Synthetic Rubber Company) was used in this study. Its molecular characteristics are  $M_n = 6.31 \times 10^4$ ,  $M_w/M_n = 1.15$ , and  $\phi_{PS} = 0.56$ , where  $M_n$  and  $M_w$  denote the number-average and the weight-average molecular weights, respectively, and  $\phi_{PS}$  is the volume fraction of the PS blocks. The composition was evaluated by a  $^1\text{H-NMR}$  measurement. Note here that this SBS sample forms well-ordered lamellar microdomains in the absence of cross-links [23].

SBS triblock copolymer, dioctyl phthalate (DOP), and (1,1-bis(*tert*-butylperoxy)-3,3,5-trimethylcyclohexane) as a cross-linking agent (peroxide) were dissolved in methylene chloride with the concentration of SBS + DOP being ca. 5 wt%. The concentration of cross-linker ( $c_x$ ) is in the range 0.5–2.0 wt% of the amount of SBS. The homogenous mixture of SBS, DOP and cross-linker was obtained by evaporating the solvent (methylene chloride) from the casting solution at room temperature. After the solvent was completely removed, the mixture obtained was further annealed for 100 min at 150 °C in order to activate the cross-linker, which cross-linked the PB chains [23–26]. The volume fraction of SBS in the SBS + DOP mixture was 0.41. Note that the order–disorder transition temperature for this mixture was determined by the SAXS technique to be 105 °C [23]. The cross-linked material was rinsed in toluene for 1 day to extract DOP and uncross-linked polymer [23]. Toluene was refreshed at least seven times for complete removal. Then, the cross-linked SBS was finally obtained by evaporating toluene from the swollen SBS materials and we obtained the as-cross-linked sample. The as-cross-linked sample undergoes microphase separation with a bicontinuous microdomain structure during the evaporation of toluene [23].

To conduct uniaxial stretching of a cross-linked SBS film at 130 °C, a lump of cross-linked SBS film was thin-sliced into films with 0.07–0.4 mm in thickness. Since the SBS film was ruptured, when the stretched film was subjected to the long-term annealing at 130 °C, we conducted the following experimental procedure. First, the SBS was stretched out at 130 °C in the heating blocks under the atmospheric condition. The degree of elongation  $\epsilon$  ( $=l/l_0$ , where  $l$  and  $l_0$  denote lengths of the SBS samples at stretched and unstretched state, respectively) for the uniaxial drawing is set to  $\epsilon = 1$ –6. Then the sample was quenched to 0 °C in ice water mixture and this is referred to as the quenched sample.

After the quenched sample was removed from a drawing device, it was then sandwiched by two pieces of glass plate. Note that sandwiching with the glass plate enabled to prevent the drawn sample from relaxing and being ruptured during the thermal annealing at 130 °C for given duration. This sample is hereafter referred to as the annealed sample.

### 2.2. SAXS measurement

To quantify the degree of ordering of the microdomain structures, we conducted SAXS experiments at the BL-10C beamline in the Photon Factory of the Research Organization for High Energy Accelerator, Tsukuba, Japan. The light source of this beamline is a bending magnet. The primary beam was monochromatized with a couple of Si(111) crystals at the wavelength being 0.149 nm and then it was focused on a detector plane by a Pt-coated bent cylindrical mirror. A one-dimensional position sensitive proportional counter (PSPC) was used to detect scattering intensities and was set vertically at a position of 1.9 m apart from the sample. The sample thickness was in the range 0.07–0.4 mm. The samples were exposed to the X-ray beam, so that the film normal is perpendicular to the propagation direction of the incident beam and at the same time it is parallel to the direction of the scattering vector  $q$  (so-called edge-view geometry). The stretching direction is perpendicular to the  $q$  vector, where the magnitude of  $q$  is defined as  $q = (4\pi/\lambda)\sin(\theta/2)$  with  $\lambda$  and  $\theta$  being the wavelength of X-rays and the scattering angle, respectively. The contribution of the air scattering was subtracted with taking account of absorption due to the sample. The contribution of the thermal diffuse scattering due to density fluctuation was further subtracted according to the conventional method [27].

## 3. Results and discussion

Fig. 1 shows the edge-view SAXS profiles ( $\log I(q)$  versus  $q$ ) measured at room temperature for the as-cross-linked, quenched, and annealed samples, where  $I(q)$  denotes the scattering intensity. The concentration of the cross-linker was 1.0 wt%. Here, the quenched sample was prepared by uniaxially stretching the cross-linked SBS at 130 °C with  $\epsilon = 6$  and subsequently quenching it to 0 °C in ice water mixture. The annealed sample was obtained by thermally annealing the quenched sample at 130 °C for 24 h under the stretched state. To avoid overlaps, the profiles except for the annealed sample were shifted vertically by factors of 2 and 4, respectively. Although it is difficult to determine the morphology for the as-cross-linked and quenched samples due to lack of a higher-order diffraction peak, a bicontinuous structure was already confirmed in our previous study [23]. For the quenched sample, it was found that the peak shifted towards a higher  $q$  region with broadening as compared to the profile for the as-cross-linked sample. Since the direction of the  $q$  vector is perpendicular

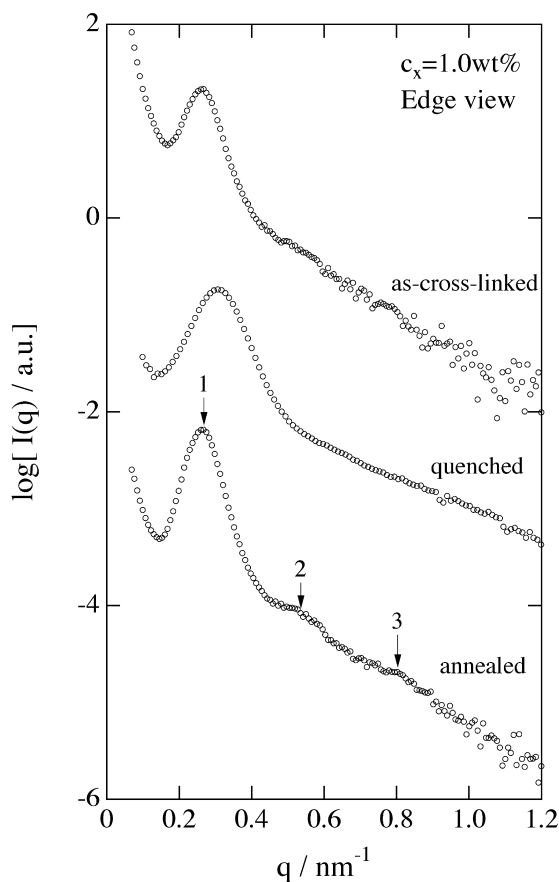


Fig. 1. Edge-view SAXS profiles measured at room temperature for the as-cross-linked, quenched, and annealed samples. The concentration of the cross-linker was 1.0 wt%. The degree of elongation  $\epsilon = 6$  for the quenched and annealed samples.

to the drawing direction, the fact that the peak shifts towards the higher  $q$  indicates a decrease in the domain size along this direction and in turn suggests deformation of the microdomains due to stretching. More details are discussed later in Fig. 3(a). On the other hand, for the annealed sample, the appearance of two higher-order peaks can be identified at relative  $q$  values of 2 and 3 with respect to the first-order peak position, which are marked with arrows in the profile. These are higher-order diffraction peaks from regularly ordered microdomains. For the annealed sample, the first-order peak shifts towards a smaller angle with sharpening, as compared to the profile for the quenched sample. Namely, regularity of the microdomain structure was improved, whereas the domain spacing recovered its original size observed for the as-cross-linked sample upon the thermal annealing.

We also conducted 2d SAXS measurements to check orientation of microdomains. Fig. 2 displays the results for: (a) as-cross-linked and (b) annealed samples, where the concentration of cross-linker was 1.5 wt% and the degree of elongation was  $\epsilon = 5$  for the annealed sample (annealed at 130 °C for 24 h). Here,  $q_x$  and  $q_y$  are perpendicular and parallel to the stretching direction. It was found

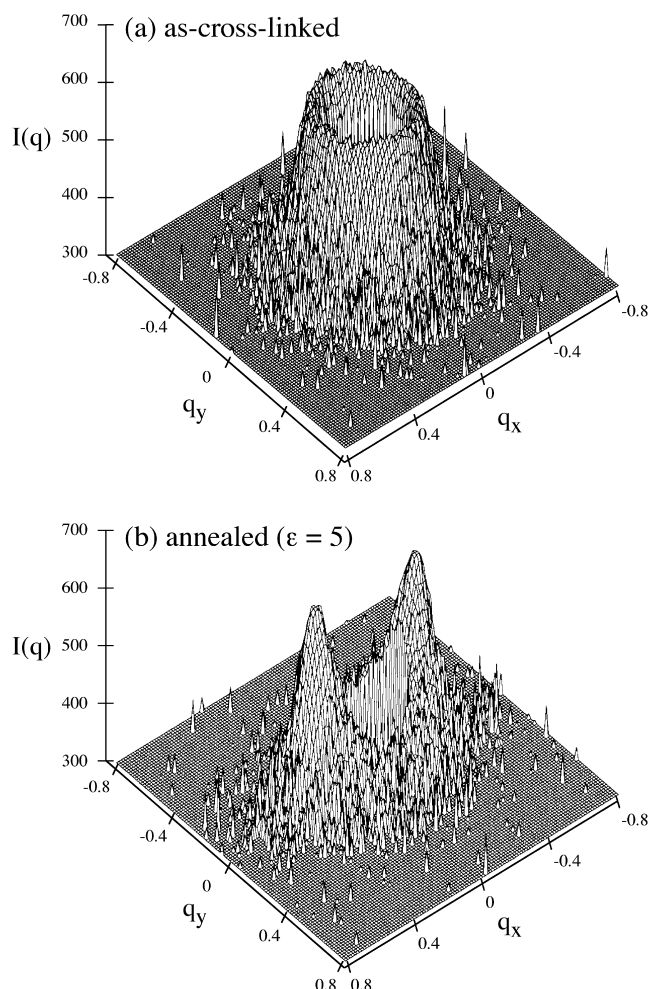


Fig. 2. Wire frame plots of the 2d-SAXS pattern measured at room temperature for: (a) as-cross-linked and (b) annealed samples, where the concentration of cross-linker was 1.5 wt% and the degree of elongation was  $\epsilon = 5$  for the annealed sample (annealed at 130 °C for 24 h). Here,  $q_x$  and  $q_y$  are perpendicular and parallel to the stretching direction, respectively.

that the isotropic SAXS pattern for the as-cross-linked sample transformed into anisotropic one for the annealed sample at the stretched state ( $\epsilon = 5$ ). Combining the results of 1d and 2d SAXS measurements, it is concluded that the lamellar-like one-dimensional regularity of microdomains is preferentially induced in the direction perpendicular to the stretching direction. Thus, not only ordering, but also orientation of microdomains took place upon the uniaxial stretching. This experimental finding is in good accord with theoretical prediction by Panyukov and Rubinstein [13], which is discussed later in more detail.

Elongation dependencies of the domain spacing ( $D$ ) in the direction perpendicular to the drawing direction and the peak width (hwhm: half-width at half-maximum) are shown in Fig. 3(a) and (b), respectively, for the as-cross-linked, quenched, and annealed samples. The concentration of the cross-linker was 1.0 wt%. Here, the domain spacing was evaluated from the first-order peak position ( $q^*$ ) using the Bragg equation ( $D = 2\pi/q^*$ ). Upon stretching, the

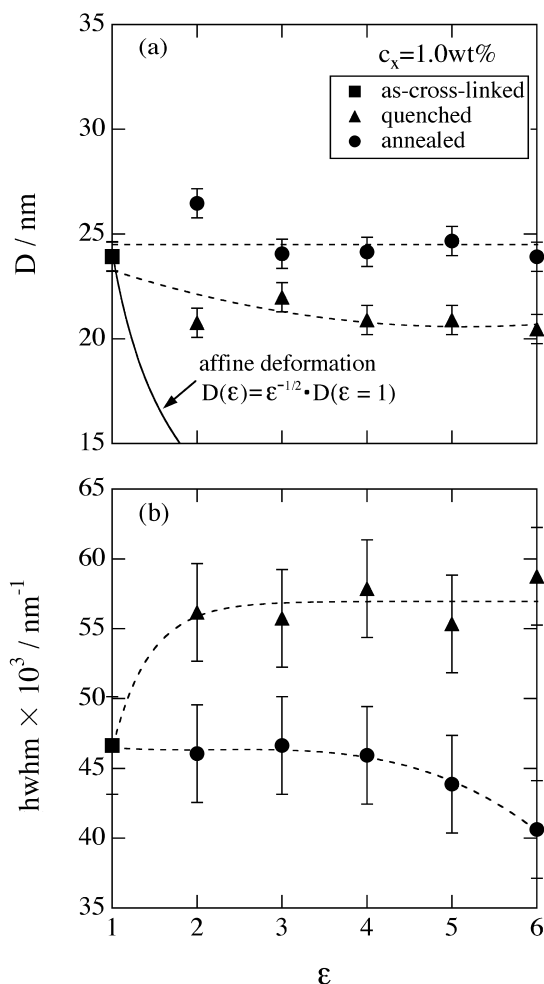


Fig. 3. Elongation dependencies of: (a) the domain spacing ( $D$ ) in the direction perpendicular to the drawing direction and (b) the peak width ( $hwhm$ ) for the as-cross-linked, quenched, and annealed samples. The concentration of the cross-linker was 1.0 wt%.

value of  $D$  for the quenched samples decreased as compared to that for the as-cross-linked sample. Although this fact suggests that the bicontinuous microdomains are readily deformed due to the extensional flow in the melt state upon the uniaxial stretching at 130 °C, the decay of  $D$  with  $\epsilon$  did not follow the affine deformation. The observed  $D$  value is much bigger than the value accounted for by the affine deformation. As for the peak width, the values for the quenched samples are about 50% increased from the value for the as-cross-linked sample. Generally, the peak width is inversely correlated with the degree of regularity of the microdomain structure. Therefore, the peak broadening upon stretching indicates that the regularity of the microdomain structure becomes worse upon stretching. The value of  $D$  is almost constant irrespective of elongation for the annealed sample. Furthermore, the domain spacing recovered its original size observed for the as-cross-linked sample. On the other hand, the peak width decreased upon annealing. The value of  $hwhm$  is almost constant irrespective of elongation below  $\epsilon = 4$ , whereas it seems to become

even slightly smaller with elongation above  $\epsilon = 4$ . Those results indicate that the microdomain structures gradually ordered upon the prolonged annealing under the stretched state with recovering its original domain spacing and the regularity of the microdomains becomes even higher under a highly stretched state.

Elongation dependencies of  $D$  and peak width are shown in Fig. 4(a) and (b), respectively, for the annealed samples ( $\epsilon \geq 2$ ) and for the as-cross-linked samples ( $\epsilon = 1$ ) for various values of cross-linker concentration ( $c_x$ ). The domain spacing shows no appreciable change with elongation and cross-linker concentration. On the other hand, the degree of regularity of the microdomain structure was comparatively better for a lower concentration of the cross-linker at a lower elongation regime below  $\epsilon = 3$ . The effect of elongation on the degree of regularity of the microdomain structure is dramatic for the case of  $c_x = 2.0$  wt% such that the regularity becomes better upon stretching, while it remains constant for  $c_x = 1.0$  or 1.5 wt%. However, it should be rather noted that the regularity of the as-cross-linked sample with  $c_x = 2.0$  wt%

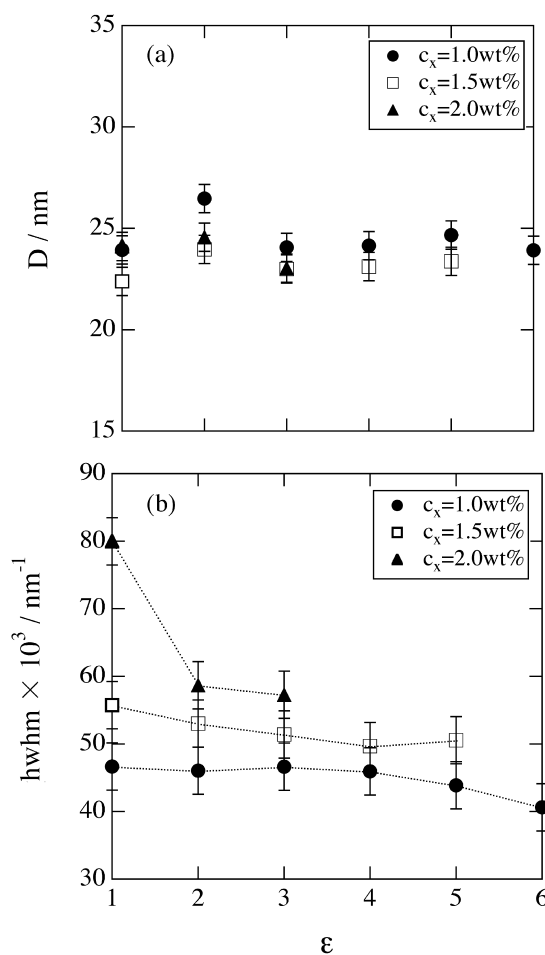


Fig. 4. Elongation dependencies of: (a) the domain spacing ( $D$ ) in the direction perpendicular to the drawing direction and (b) the peak width ( $hwhm$ ) for the annealed samples with various values of cross-linker concentration ( $c_x$ ).

was much worse. It may be because the microdomain formation was prevented by the chemical cross-links in this sample cross-linked with an extremely high degree of cross-linking. Upon stretching, the value of the peak width for  $c_x = 2.0$  wt% approached the level for other samples. Here, it is noted that the cross-linked samples with  $c_x$  below 1.75 wt% were found to suffer the melt fracture at 130 °C under the dynamic deformation with a strain amplitude of 0.01 in our previous study [24]. This result indicates that the cross-linking density for  $c_x < 1.75$  wt% was not effective enough. On the other hand, the sample with  $c_x = 2.0$  wt% was found to behave like cross-linked rubber and did not melt fracture above  $T_{g,PS}$ . Therefore, it might be expected that the regularity of the microdomains becomes better than the other samples at a higher elongation regime above  $\epsilon = 3$ , although it was not observed because of the experimental difficulty. Namely, the melt fracture took place by the prolonged annealing under such a highly stretched state.

We applied the similar analysis to the second-order peak. However, an appreciable difference could not be obtained. Therefore, we calculated the correlation function  $\langle \gamma(r) \rangle$  from the whole scattering function  $I(q)$  by the following equation [28]:

$$\langle \gamma(r) \rangle = \frac{\int_0^\infty I(q) (\cos qr) q^2 dq}{\int_0^\infty I(q) q^2 dq} \quad (1)$$

As shown in Fig. 2(b), preferential orientation of microdomains was resulted from uniaxial stretching, irrespective of the extent of deformation. Therefore, Eq. (1), that is, applied to structures having a one-dimensional period was used for all of the stretched samples to evaluate the correlation function. Generally, extrapolation of the scattering intensity  $I(q)$  in lower and higher  $q$  regions are required to conduct integration in Eq. (1). However, it is an issue how to extrapolate. We are aware of an artifact due to it and prefer to calculate the correlation function without extrapolation to avoid any unfavorable artifact. It is therefore important to compare results with and without extrapolation. The Guinier's law describes the scattering function in a low  $q$  region as  $I(q) \sim \exp(-kq^2)$ . For strongly segregated block copolymers, the interface of the microdomains is narrow and the Porod's law holds. Thus, the scattering intensity in a high  $q$  region was extrapolated with  $I(q) \sim q^{-4}$ . Fig. 5(a) demonstrates the extrapolation in broken curve for the measured data (in solid curve). Fig. 5(b) compares the obtained results for the correlation function with and without the extrapolation, as shown, respectively, in broken and solid curves. Although peak positions are seemed to be unaffected, the overall curves are not identical to each other. As discussed later, the height of first-order correlation peak is evaluated as an index of microdomain regularity. According to our definition of the peak height schematically shown in the inset of Fig. 7, no difference in the peak height

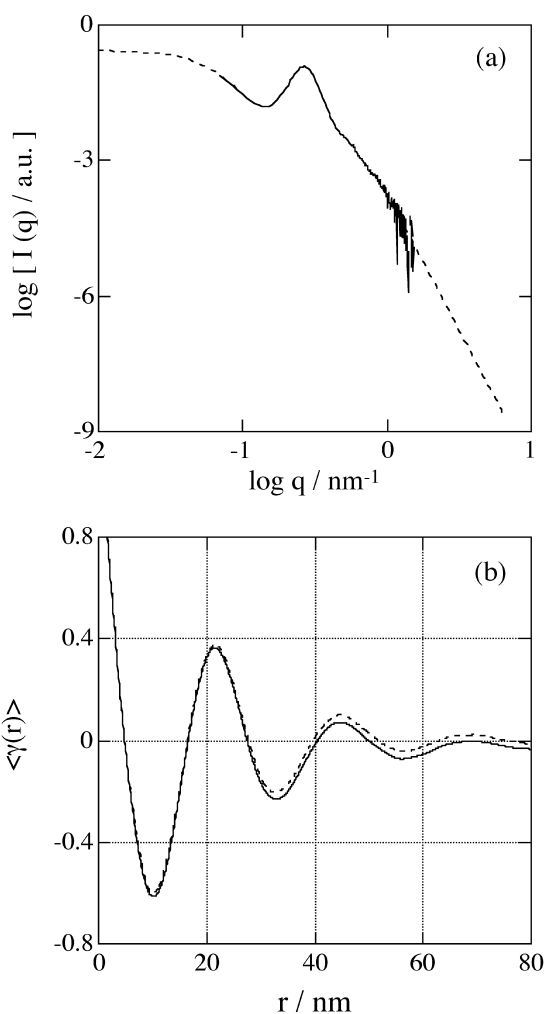


Fig. 5. (a) Extrapolation of the scattering function  $I(q)$  shown in broken curve for the measured data (in solid curve). (b) Comparison of the correlation function calculated with and without the extrapolation, as shown, respectively, in broken and solid curves.

attributed to the extrapolation was found. Therefore, extrapolation is not necessary exclusively for our purpose, and we do not conduct extrapolation hereafter to calculate the correlation function.

Fig. 6 shows the correlation function for the annealed samples with various values of  $\epsilon$ . For all samples, three distinct peaks can be identified around  $r = 28, 57$ , and  $87$  nm, which are roughly equal to the domain spacing and its double and triple, respectively. The peak becomes broader and the peak around  $r = 87$  nm disappeared, when the cross-linker concentration was increased for a given value of  $\epsilon$ . Namely, the strong correlation of the microdomain structures weakened due to ill development of microphase separation [23]. Upon stretching, the peak becomes sharper, even for the higher cross-linker concentration. To discuss more quantitatively, we extracted the peak height as an index of correlation strength. As schematically shown in the inset of Fig. 7, the peak height is defined as the height from the bottom to the top of the first-order

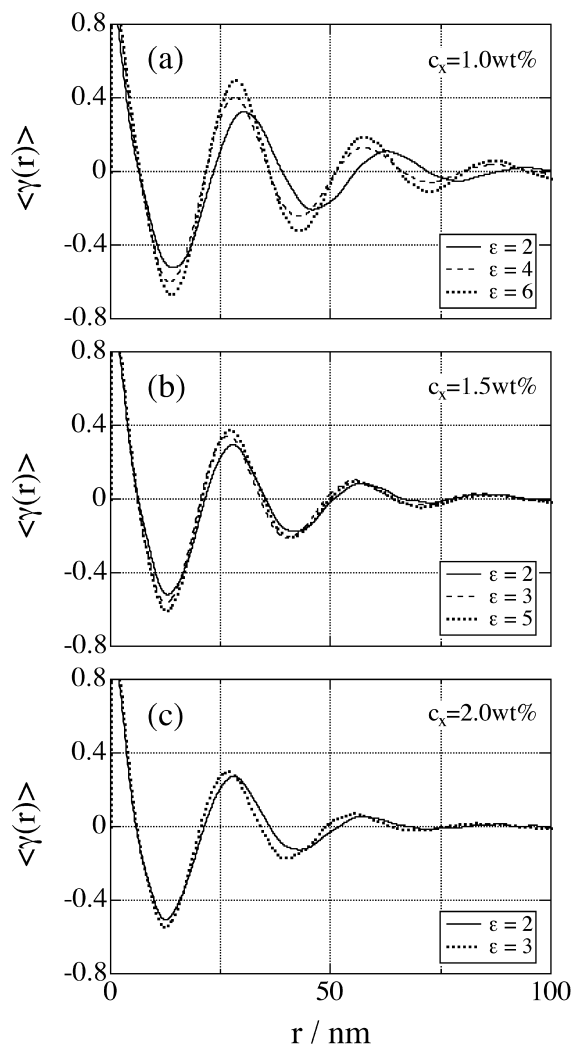


Fig. 6. Correlation function for the as-cross-linked and annealed samples for various  $c_x$  values of: (a) 1.0 wt%, (b) 1.5 wt%, and (c) 2.0 wt%.

correlation peak. Fig. 7 shows elongation dependence of the peak height for annealed samples. The peak height increased with an increase of elongation. The overall tendency of the result is indeed in good accord with that of the width of the first-order peak (Fig. 4(b)).

It has been revealed in our previous study that no appreciable lamellar-like ordering was resulted from prolonged thermal annealing even up to 50 h without stretching samples, when the cross-linker concentration was higher than 1.0 wt% (see fig. 12 in Ref. [23]). This is because heavily cross-linked networks prevent the SBS sample from undergoing microphase separation with long-range order. Therefore, the earlier-described results in the present study clearly address significant role of uniaxial stretching to generate the long-range order in such the cross-linked SBS sample. According to theoretical consideration by Panyukov and Rubinstein [13], quenched random elastic forces act on the microdomains and these forces destroy the long-range order of microdomains in an undeformed sample. Upon uniaxially stretching the sample,

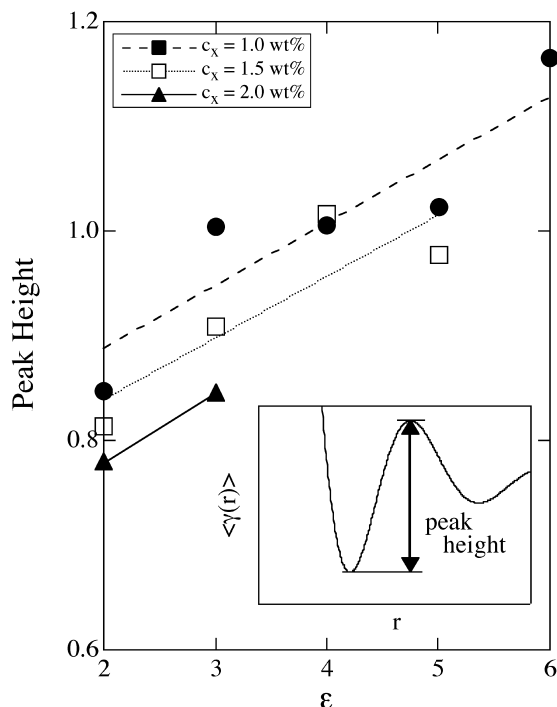


Fig. 7. Elongation dependencies of the peak height for the annealed samples. The peak height is defined as the height from the bottom to the top of the first-order correlation peak (inset).

anisotropic deformation of the cross-linked network results in symmetry breaking and hence the long-range order recovers in an anisotropic manner. As is clearly demonstrated in their paper (fig. 4 in Ref. [13]), the anisotropic long-range order is induced perpendicular to the stretching direction, and its extent is increased with an increase of the degree of deformation of the cross-linked network. In fact, we observed experimentally similar results as shown typically in Fig. 2.

#### 4. Conclusions

We examined strain-induced ordering of microdomain structures in cross-linked SBS samples by the SAXS technique. After the PB blocks of SBS samples were chemically cross-linked in the disordered state, we conducted uniaxial stretching of the cross-linked samples at 130 °C and subsequent thermal annealing under stretched state for 24 h. The initial morphology was represented by ill-ordered microdomain structures with a bicontinuous feature owing to the presence of the chemical cross-links between the PB chains. For the quenched sample, the regularity of the microdomain structure becomes worse upon stretching above  $T_{g,PS}$ , as compared to the as-cross-linked samples. However, the regularity was improved in turn upon thermal annealing under the stretched state. It was further found that the ordering proceeded more for the case of the higher strain.

## Acknowledgements

Synchrotron SAXS experiments were conducted under the approval of the Photon Factory Advisory Committee (Proposal Number 97G230).

## References

- [1] Molau GE. In: Aggarwal SL, editor. Block polymers. New York: Plenum Press, 1970.
- [2] Masten MW, Bates FS. *Macromolecules* 1996;29:1091.
- [3] Khandpur AK, Forster S, Bates FS, Hamley IW, Ryan AJ, Bras W, Almdal K, Mortensen K. *Macromolecules* 1995;26:8796.
- [4] Sakurai S. *Trends Polym Sci* 1995;3:90.
- [5] Legge NR, Holden G, Schroeder HE. *Thermoplastic elastomers*. 2nd ed. Munich: Hanser, 1996.
- [6] Yu MJ, Dubois P, Teyssie P, Jerome R. *Macromolecules* 1996;19:6090.
- [7] Weidisch R, Stamm M, Michler GH, Fischer H, Jerome R. *Macromolecules* 1999;3:742.
- [8] Dair BJ, Honeker C, Alward DB, Avgeropoulos A, Hadjichristidis N, Fetters LJ, Capel M, Thomas EL. *Macromolecules* 1999;24:8145.
- [9] Weidisch R, Michler GH, Arnold M. *Polymer* 2000;41:2231.
- [10] Weidisch R, Michler GH, Arnold M, Hofmann S, Stamm M. *Polymer* 1999;40:1191.
- [11] Winey KI, Patel SS, Larson RG, Watanabe H. *Macromolecules* 1993;26:2542.
- [12] Okamoto S, Saijo K, Hashimoto T. *Macromolecules* 1994;26:5271.
- [13] Panyukov S, Rubinstein M. *Macromolecules* 1996;29:8220.
- [14] Sakurai S, Aida S, Okamoto S, Ono T, Imaizumi K, Nomura S. *Macromolecules* 2001;11:3672.
- [15] Scott D, Waddon AJ, Lin YG, Karasz FE, Winter HH. *Macromolecules* 1992;16:4175.
- [16] Morrison FA, Mays JW, Muthukumar M, Nakatani AI, Han CC. *Macromolecules* 1993;26:5271.
- [17] Daniel C, Hamley IW, Mortensen K. *Polymer* 2000;41:9239.
- [18] Jackson CL, Barnes KA, Morrison FA, Mays JW, Nakatani AI, Han CC. *Macromolecules* 1995;3:713.
- [19] Daniel C, Hamley IW, Mortensen K. *Polymer* 2000;41:9239.
- [20] Kotaka T, Okamoto M, Kojima A, Kwon YK, Nojima S. *Polymer* 2001;7:3223.
- [21] Almdal K, Koppi KA, Bates FS. *Macromolecules* 1993;15:4058.
- [22] Okamoto S, Saijo K, Hashimoto T. *Macromolecules* 1994;27:3753.
- [23] Sakurai S, Iwane K, Nomura S. *Macromolecules* 1993;26:5479.
- [24] Sakurai S, Aida S, Nomura S. *Polymer* 1999;40:2071.
- [25] Hashimoto T, Takenaka M, Jinnai H. *Polym Commun* 1989;30:177.
- [26] Jinnai H, Hasegawa H, Hashimoto T, Briber RM, Han CC. *Macromolecules* 1993;26:907.
- [27] Sakurai S, Umeda H, Furukawa C, Irie H, Nomura S, Lee HH, Kim JK. *J Chem Phys* 1998;108:4333.
- [28] Strobl G. *The physics of polymer*. Berlin: Springer, 1995.